

Improved seasonal prediction of UK regional precipitation using atmospheric circulation

Article

Accepted Version

Baker, L. ORCID: <https://orcid.org/0000-0003-0738-9488>,
Shaffrey, L. ORCID: <https://orcid.org/0000-0003-2696-752X>
and Scaife, A. A. (2018) Improved seasonal prediction of UK regional precipitation using atmospheric circulation. *International Journal of Climatology*, 38 (S1). e437-e453. ISSN 0899-8418 doi: <https://doi.org/10.1002/joc.5382> Available at <https://centaur.reading.ac.uk/73964/>

It is advisable to refer to the publisher's version if you intend to cite from the work. See [Guidance on citing](#).

Published version at: <http://onlinelibrary.wiley.com/doi/10.1002/joc.5382/full>

To link to this article DOI: <http://dx.doi.org/10.1002/joc.5382>

Publisher: John Wiley & Sons

All outputs in CentAUR are protected by Intellectual Property Rights law, including copyright law. Copyright and IPR is retained by the creators or other copyright holders. Terms and conditions for use of this material are defined in the [End User Agreement](#).

www.reading.ac.uk/centaur

CentAUR

Central Archive at the University of Reading

Reading's research outputs online

Improved seasonal prediction of UK regional precipitation using atmospheric circulation

L. H. Baker^{*1}, L. C. Shaffrey¹, and A. A. Scaife²

¹NCAS Climate, Department of Meteorology, University of Reading, Reading, UK

²Met Office Hadley Centre, Exeter, UK

*Correspondence to: Department of Meteorology, University of Reading, P.O. Box 243, Reading, RG6 6BB, UK. l.h.baker@reading.ac.uk

Keywords: precipitation, atmospheric circulation, seasonal forecasting, down-scaling

Funding: LHB was supported by the NERC project IMPETUS (ref. NE/L010488/1). AAS was supported by the Joint DECC/Defra Met Office Hadley Centre Climate Programme (GA01101).

Abstract

The aim of this study is to further our understanding of whether skilful seasonal forecasts of the large-scale atmospheric circulation can be downscaled to provide skilful seasonal forecasts of regional precipitation. A simple multiple linear regression model is developed to describe winter precipitation variability in nine UK regions. The model for each region is a linear combination of two mean sea-level pressure (MSLP)-based indices which are derived from the MSLP correlation patterns for precipitation in north-west Scotland and south-east England. The first index is a pressure dipole, similar to the North Atlantic Oscillation but shifted to the east; the second index is the MSLP anomaly centred over the UK. The multiple linear regression model describes up to 76% of the observed precipitation variability in each region, and gives higher correlations with precipitation than using either of the two indices alone. The Met Office’s seasonal forecast system (GloSea5) is found to have significant skill in forecasting the two MSLP indices for the winter season, in forecasts initialised around the start of November. Applying the multiple linear regression model to the GloSea5 hindcasts is shown to give improved skill over the precipitation forecast by the GloSea5, with the largest improvement in Scotland.

1 Introduction

In recent years, the UK has experienced several extreme seasonal precipitation events, with instances of heavy rain leading to flooding in some regions (e.g. winter 2013–2014; [Huntingford *et al.*, 2014](#); [Kendon and McCarthy, 2015](#); [Muchan *et al.*, 2015](#); [Sibley *et al.*, 2015](#)), and periods of low precipitation leading to drought in others (e.g. the 2010–2012 drought; [Kendon *et al.*, 2013](#); [Parry *et al.*, 2013](#)). The ability to forecast the risk of such events on seasonal timescales enables forward planning and the implementation of measures to mitigate the effects of these events on society.

There have been recent advances in the capability of seasonal forecasting for the North Atlantic and Europe. For example, [Scaife *et al.* \(2014\)](#) demonstrated that the GloSea5 system was able to skilfully forecast the wintertime North Atlantic Oscillation (NAO) from forecasts initialised around the start of November. However, it still remains extremely challenging to skilfully forecast the details of European weather on seasonal timescales.

One way to address this challenge is to utilise the observed relationships between the NAO and European weather. The NAO is often defined as the mean sea-level pressure (MSLP) difference between the Azores High and the Icelandic Low (e.g. [Hurrell *et al.*, 2003](#)) and is a well-known driver of the weather in the UK and Northern Europe. When the NAO is positive, the North Atlantic jet is stronger, the UK and Northern Europe experience milder temperatures, stronger westerly winds, and more frequent passage of extratropical storms with associated precipitation. When the NAO is negative, the UK and Northern Europe experiences colder temperatures, with more frequent episodes of anticyclonic blocking, weaker winds and generally drier conditions.

This approach was adopted by [Scaife *et al.* \(2014\)](#), who showed that higher correlation skill scores are obtained for observed winter storminess, temperature and windspeed over much of Northern Europe when using the GloSea5 prediction of the NAO rather than the direct GloSea5 predictions of these weather

49 variables. Similarly, [Svensson *et al.* \(2015\)](#) made use of the GloSea5 NAO fore-
50 cast skill by including the NAO index as an input to a river flow model. They
51 showed that using the NAO index from GloSea5 seasonal forecasts improved the
52 skill of winter river flow forecasts for the UK. [Palin *et al.* \(2015\)](#) demonstrated
53 that the GloSea5 winter NAO forecasts can be used to provide skilful forecasts
54 of winter impacts on UK transport. [Karpechko *et al.* \(2015\)](#) found that skil-
55 ful forecasts of Baltic Sea maximum ice extent could be obtained by using the
56 GloSea5 winter NAO forecasts, which were more skilful than using explicit sea
57 ice forecasts.

58 One key question is whether regional winter precipitation over the UK is pri-
59 marily driven by the NAO or whether other patterns of atmospheric circulation,
60 such as the East Atlantic Pattern (EAP), are also important. The EAP is char-
61 acterised by a MSLP anomaly centred to the east of the central North Atlantic
62 ([Barnston and Livezey, 1987](#)) and can affect the position of the North Atlantic
63 jet ([Woollings *et al.*, 2010](#)). The positive phase of the EAP is associated with a
64 low pressure anomaly in the North Atlantic, with warmer temperatures in west-
65 ern Europe and increased precipitation to the south of, and collocated with,
66 the low pressure centre. In the negative phase of the EAP, the high pressure
67 anomaly in the North Atlantic is associated with a northward displacement of
68 the jet and increased anticyclonic blocking in southwestern Europe.

69 The summer counterpart to the NAO, the summer NAO (SNAO) has a
70 more northward position and smaller spatial extent, with MSLP centres ap-
71 proximately over Greenland and the UK ([Folland *et al.*, 2009](#)). The positive
72 phase of the SNAO is associated with high pressure over the UK and a stronger
73 jet to the north, with the UK experiencing warmer, generally drier conditions;
74 the negative phase has lower pressure over the UK and a weaker jet to the north,
75 with the UK experiencing cooler, generally wetter conditions. In summer, the
76 EAP pressure anomaly is weaker than in winter and is located further east, just
77 to the west of the UK.

78 The relationship between regional precipitation and atmospheric circulation
79 was investigated by [Wilby *et al.* \(1997\)](#), who showed that for winters with a
80 strong positive NAO index, the west of Scotland had the strongest positive
81 rainfall anomalies, while eastern England had negative rainfall anomalies. In
82 contrast, in years with a strong negative NAO index, eastern England had posi-
83 tive rainfall anomalies while the west of Scotland had negative rainfall anoma-
84 lies. [Murphy and Washington \(2001\)](#) found that in winter an index similar
85 to the NAO (with slightly shifted centres) controlled the north-west/south-east
86 precipitation gradient, while a second mode of atmospheric variability, with cen-
87 tres over Scotland and Madeira, controlled the precipitation amount over the
88 UK. In summer a MSLP index with centres over Scotland and Greenland con-
89 trolled the precipitation over the whole UK, but not the north-west/south-east
90 gradient. [Lavers *et al.* \(2010\)](#) looked at the relationship between precipitation
91 and river flow at ten observation stations across the UK, and different atmo-
92 spheric fields. They found that the relative importance of the different quantities
93 varied spatially and temporally. For stations in the north-western UK, winter
94 precipitation is correlated with westerly winds and a MSLP dipole similar to
95 the NAO. For stations in the south-east of England, winter precipitation is cor-
96 related with negative MSLP anomalies centred over the UK and westerly winds
97 to the south. Similarly [Folland and Woodcock \(1986\)](#) used MSLP patterns to
98 forecast half-monthly rainfall in different UK regions, and show a correlation

99 of -0.80 between MSLP and precipitation in South-West England and South
100 Wales in the first half of January. [Folland *et al.* \(2015\)](#) found a similarly strong
101 correlation of -0.78 between the English Lowlands (the south-east of England)
102 rainfall and MSLP anomalies centred over this region for the winter half-year.

103 Other studies used Lamb Weather Types (LWTs, [Lamb, 1950](#)) to cate-
104 gorise atmospheric circulation patterns and linked them with UK weather.
105 [Jones *et al.* \(2014\)](#) studied relationships between UK precipitation and objec-
106 tively defined LWTs ([Jones *et al.*, 2013](#)). They found significant positive (neg-
107 ative) correlations between England and Wales total seasonal precipitation and
108 the cyclonic (anticyclonic) LWTs in all four seasons. The LWTs can also
109 be expressed in terms of the mean flow direction and strength and vorticity
110 ([Jenkinson and Collison, 1977](#)). [Osborn *et al.* \(1999\)](#), [Turnpenny *et al.* \(2002\)](#)
111 and [Jones *et al.* \(2013\)](#) looked at the relationship between regional precipita-
112 tion and these circulation measures. They found that in south-east England the
113 vorticity had the strongest link with the precipitation amount in all seasons,
114 with high vorticity and cyclonic conditions generally leading to more precipi-
115 tation. In north-west England and western Scotland the precipitation amount
116 was most strongly influenced by flow strength, with stronger flows resulting in
117 more precipitation.

118 The aim of this study is to further our understanding of whether skilful
119 seasonal forecasts of the large-scale atmospheric circulation can be statistically
120 downscaled to provide skilful seasonal forecasts of regional precipitation. This
121 will be addressed by:

- 122 1. investigating the atmospheric circulation patterns associated with winter
123 precipitation in different UK regions;
- 124 2. using these circulation patterns to produce a simple statistical downscaling
125 method to describe UK regional precipitation variability and;
- 126 3. applying this downscaling methodology to the GloSea5 seasonal forecast
127 data to provide improved seasonal forecasts of UK regional precipitation.

128 Section 2 describes the datasets used. In Section 3 the relationship between
129 precipitation in different UK regions, and the relationship between regional
130 precipitation and MSLP, are discussed. In Section 4 a multiple linear regres-
131 sion model is developed for UK regional precipitation, which is then applied to
132 seasonal forecast data in Section 5 to test its capability at providing regional
133 precipitation forecasts. Finally, Section 6 gives a summary of the results and a
134 discussion of applications of this methodology.

135 2 Methodology and data

136 The precipitation observation data used in this study is the HadUKP UK re-
137 gional precipitation series ([Alexander and Jones, 2000](#)). Data is available for 9
138 regions of coherent precipitation variability (as defined by [Gregory *et al.* \(1991\)](#);
139 see maps in Fig. 1), for the period 1931 to present for Scotland and Northern
140 Ireland, and the period 1873 to present for England and Wales. Only data
141 between 1931 and 2012 is used in this study, for consistency between regions.
142 The long period over which this data is available, and the fact that it is divided
143 into predetermined coherent regions, makes it a suitable choice for this study.

144 The precipitation data is derived from observed daily precipitation data from
145 a selection of quality-controlled rainfall stations within each region, which are
146 combined to give area average daily and monthly precipitation values for each
147 region. Monthly means are used here, since daily data has been found to be too
148 noisy in similar studies (Lavers *et al.*, 2010, 2013). In addition to this regional
149 precipitation dataset, the Met Office’s UKCP09 gridded precipitation dataset
150 (Met Office *et al.*, 2017) is also used. This includes monthly mean precipitation
151 observations on a high-resolution 5km \times 5km grid over the UK, and is available
152 from January 1910 to December 2014.

153 The MSLP observation dataset used is HadSLP2r (Allan and Ansell, 2006).
154 This is a gridded dataset created using marine and land observations, which are
155 blended and interpolated onto a 5° \times 5° regular grid. The HadSLP2r dataset
156 extends back to the year 1850, and therefore covers the period studied in this
157 paper.

158 The seasonal hindcast data is from the Met Office Global Seasonal forecast
159 system, GloSea5 (MacLachlan *et al.*, 2015). This is a global ensemble forecast
160 system with 24 ensemble members. The hindcast set covers the period winter
161 1992–1993 to winter 2011–2012, and is the same hindcast dataset as used by
162 Scaife *et al.* (2014). Hindcasts were initialised on 25 October, 1 November and
163 9 November in each year, with eight members for each start date; members from
164 the same start date differ from each other by applying a stochastic physics pa-
165 rameterisation. The model has a resolution of 0.83° longitude by 0.55° latitude,
166 85 levels in the vertical, with model top at 85km, and a relatively high-resolution
167 ocean (\sim 0.25° horizontally, 75 vertical levels) with interactive sea-ice. For con-
168 sistency with observed MSLP, the model MSLP fields have been regridded to
169 the HadSLP2 5° \times 5° grid. For comparison between GloSea5 precipitation and
170 the UKCP09 observed precipitation, the UKCP09 is regridded to the GloSea5
171 grid and a land-sea mask applied to remove points where at least 50% of the
172 gridbox is ocean.

173 Throughout this paper ‘winter’ is defined as the average of December, Jan-
174 uary and February, and referred to as DJF, and ‘summer’ is defined as the
175 average of June, July and August, and referred to as JJA. Individual winters
176 are referred to by the year corresponding to the December at the start of the
177 season (e.g. winter 2011–12 is referred to as winter 2011).

178 3 Regional precipitation variability in the UK

179 The aim of this section is to explore the relationships between precipitation
180 in each UK region, and the associated atmospheric circulation patterns. The
181 seasonal precipitation for winter and summer for each of the HadUKP regions is
182 shown in Fig. 1 and Table 1. In both seasons, there is a clear north-west/south-
183 east gradient in precipitation, with more precipitation received in the north-
184 western regions than the south-eastern regions. The Northern and Southern
185 Scotland regions (NS and SS respectively) receive the most precipitation in
186 both summer and winter, with more than double the amount in winter than
187 received by South-East and Central England (SEE and CE respectively). South-
188 West England (SWE) receives a large amount of precipitation in winter, but
189 considerably less in summer. East Scotland (ES) is substantially drier than
190 NS, despite their close locations. Regions in the east have similar precipitation

191 totals in summer and winter, while regions in the west have more precipitation
192 in winter.

193 To investigate the north-west/south-east gradient further, Figs. 2(a,c) show
194 the winter and summer correlations between precipitation in NS and precipita-
195 tion in each region, while Figs. 2(b,d) show correlations between precipitation
196 in SEE and precipitation in each region; the correlations are given in detail in
197 Table 1. These two regions were chosen since they are at opposite ends of the
198 domain, and because the timeseries of precipitation in each of these regions are
199 not significantly correlated in either season. NS is strongly correlated with SS
200 in both seasons (Figures 2a and c), but the correlation rapidly weakens further
201 to the south. NS also has a relatively low correlation with ES in both sea-
202 sons, despite ES being directly to the east of NS. This is due to the so-called
203 ‘rain shadow’ effect (Weston and Roy, 1994; Fowler *et al.*, 2005; Svensson *et al.*,
204 2015), whereby regions to the east of mountain ranges receive considerably less
205 precipitation under westerly flow than occurs to the west. Correlations with
206 SEE are generally stronger and more widespread than for NS (Figures 2b,d).
207 The strongest correlations with SEE are seen in the two bordering regions (SWE
208 and CE) while the weakest SEE correlations are with NS and SS. The summer
209 correlations between regions are similar to the winter correlations. However,
210 in summer there is more spatial coherence across the country than in winter,
211 with stronger correlations seen in summer between more remote regions than in
212 winter. The low correlations between regions at opposite ends of the UK might
213 indicate that precipitation in each region has different atmospheric drivers.

214 Figure 3 shows correlation maps of winter mean MSLP with precipitation in
215 each UK region. There are substantial differences in spatial patterns between
216 north-western and south-eastern regions of the UK. The NS correlation pattern
217 (Fig. 3a) has a north-south pressure dipole, and resembles the positive phase
218 of the NAO but with centres shifted to the east. Over the UK, there is a
219 strong meridional pressure gradient, corresponding to westerly wind anomalies.
220 Periods with positive precipitation anomalies in NS are therefore associated
221 with a stronger North Atlantic jet stream, stronger westerlies and the passage of
222 more low pressure systems and associated fronts across the norther UK. Periods
223 with negative precipitation anomalies in NS are associated with easterly wind
224 anomalies over the UK, corresponding to a weaker or meandering North Atlantic
225 jet stream, and typically associated with more frequent atmospheric blocking
226 patterns. SS shows a similar correlation pattern to that of NS but with slightly
227 weaker magnitude (Fig. 3b).

228 In contrast, the SEE correlation pattern (Fig. 3i) has a region of negative
229 correlations, corresponding to a low pressure anomaly, centred over the UK. This
230 resembles the EA pattern (Barnston and Livezey, 1987) but with the area of
231 strongest correlation centred further to the east, over the UK. High precipitation
232 anomalies in SEE therefore occur when there is a low pressure anomaly centred
233 over the UK, with the jet passing roughly across the centre of the UK. Low
234 precipitation anomalies in SEE are associated with a blocking pattern over the
235 UK and western Europe. North-East England (NEE) and CE show similar
236 correlation patterns to SEE (Figs. 3f and h), although the correlations are
237 slightly weaker. The correlation patterns for Northern Ireland (NI) and North-
238 West England (NWE) (Figs. 3d and e) have a north-south pressure dipole like
239 NS, but shifted further south, meaning that the low pressure part sits partly
240 over the UK, and the westerly wind anomalies are located over northern Spain.

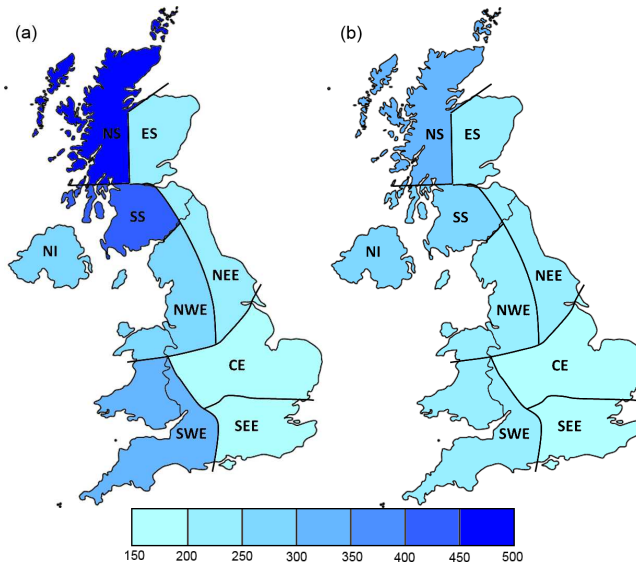


Figure 1: Maps of HadUKP observed regional precipitation, showing average total precipitation (in mm) in each region in (a) winter and (b) summer, for the period 1931–2011.

241 Therefore NI and NWE have elements of both the NS and SEE correlation
 242 patterns. SWE has a similar correlation pattern to SEE (Fig. 3g) but with
 243 the low pressure centred a little further north, while ES (Fig. 3c) has generally
 244 weaker correlations, and the low centre further to the north-east.

245 Inspection of composites of the ten wettest and driest years for each region
 246 (not shown) show that these MSLP patterns are roughly symmetric for the wet
 247 and dry cases, with only small variations in the locations of high and low MSLP
 248 anomaly centres.

249 Equivalent correlation maps are shown for summer in Fig. 4. NS shows a
 250 region of low pressure centred to the north of the UK and west of Norway (Fig.
 251 4a). All other regions show a MSLP dipole with high positive correlations over
 252 Greenland and negative correlations centred just to the east of the UK; this
 253 pattern resembles the SNAO (Folland *et al.*, 2009).

254 The above results show that in both winter and summer, the seasonal-mean
 255 precipitation in regions in the north-west and south-east of the UK are not
 256 significantly correlated, and that they are associated with different atmospheric
 257 circulation patterns.

258 4 Downscaling atmospheric drivers to estimate 259 UK regional precipitation

260 In this section the links between precipitation and MSLP circulation patterns
 261 discussed in Section 3 are used to derive a simple multiple linear regression model
 262 to estimate winter precipitation in each region based on historical observations.
 263 Only winter is considered here, since the aim is to derive a model that can be

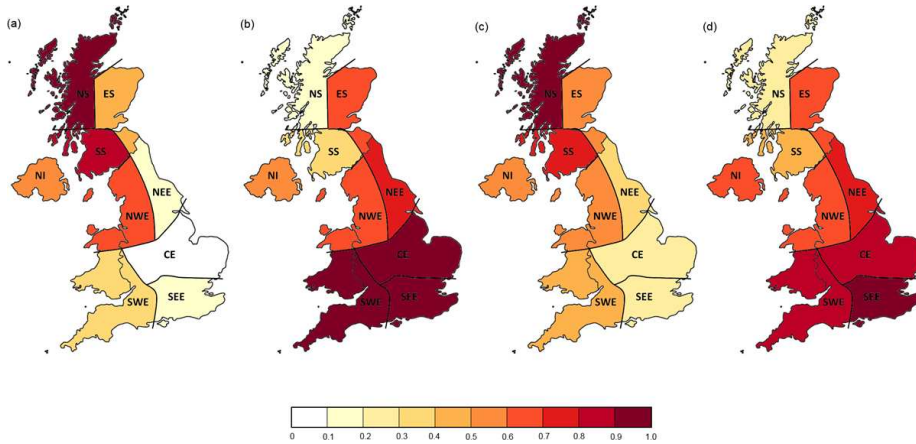


Figure 2: Maps showing seasonal correlations of HadUKP observed regional precipitation, for the period 1931–2011. Panels show correlations between each region and (a,c) NS, (b,d) SEE, in (a,b) DJF and (c,d) JJA.

264 developed for seasonal prediction, and currently the known skill of GloSea5 for
 265 the North Atlantic region is only in winter. The potential to develop a similar
 266 methodology for summer is discussed in Section 6.

267 Using the correlations discussed in Section 3, it is possible to derive a simple
 268 multiple linear regression model to estimate the winter precipitation in each UK
 269 region, making use of the fact that NS and SEE precipitation are uncorrelated
 270 and driven by different atmospheric patterns of variability. Informed by the
 271 MSLP correlation maps in Figs. 3a and i, two MSLP indices are constructed
 272 that represent these atmospheric patterns. For NS precipitation, the maximum
 273 correlation value is located in North Africa, at 35°N , 5°W , and the minimum is
 274 over the ocean to the north of the UK, at 70°N , 5°W . We construct the index
 275 MSLP_{NSI} , defined as the standardised (i.e. centred about the time-mean value
 276 and divided by the standard deviation over the timeseries) MSLP difference
 277 between the southern point and the northern point (i.e. similar to the NAO
 278 index). For SEE, there is a strong negative correlation centred over the UK.
 279 We therefore construct a MSLP index based only on MSLP at this point. We
 280 define the index MSLP_{UK} as the standardised mean MSLP anomaly in a box
 281 centred over the UK (50°N – 60°N , 10°W – 5°E). The correlation between the two
 282 indices MSLP_{NSI} and MSLP_{UK} in the period 1931–2011 is very small and not
 283 significant (-0.06).

284 To construct the multiple linear regression model, a training period (1931–
 285 1991) is used, and a later period (1992–2011) is used to evaluate the model.
 286 Figure 5a shows the correlation between winter precipitation in each region and
 287 MSLP_{NSI} and MSLP_{UK} in the training period. Precipitation in NS, SS, NI
 288 and NWE is significantly correlated with MSLP_{NSI} (blue bars), while precipita-
 289 tion in all regions except for NS is significantly correlated with MSLP_{UK} (green
 290 bars). The geographical distribution of these correlations is shown in Fig. 6.
 291 The four regions where precipitation is significantly correlated with MSLP_{NSI}
 292 are in the north-west of the UK, with the highest correlation in NS (Fig 6a).
 293 Correlations between precipitation and MSLP_{UK} are larger in the south of the

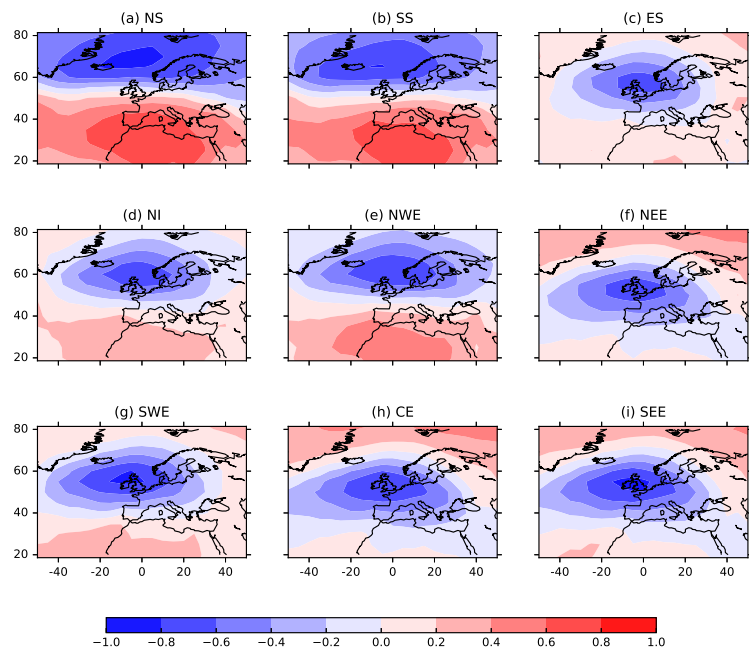


Figure 3: Maps of observed correlation between winter MSLP and winter precipitation in each of the HadUKP regions, for the period 1931–2011.

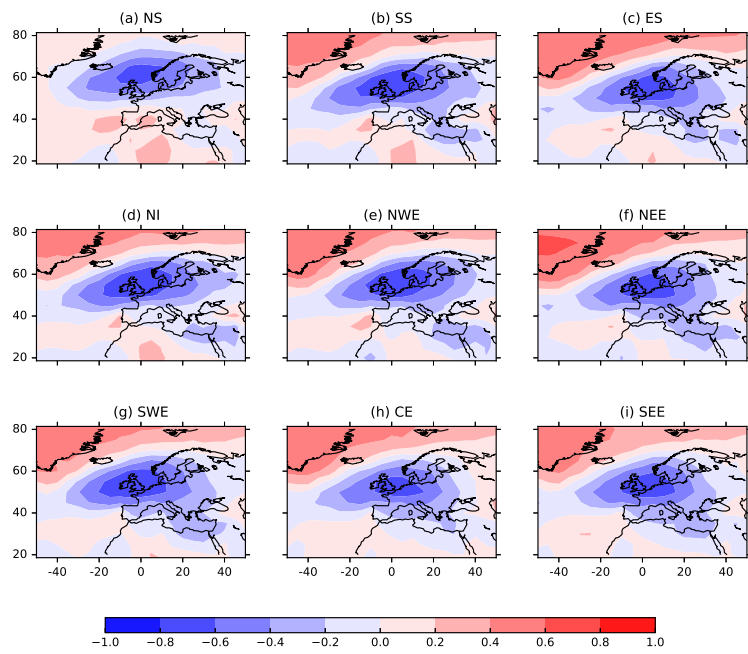


Figure 4: Maps of observed correlation between summer MSLP and precipitation in each of the HadUKP regions, for the period 1931–2011.

294 UK, with the highest correlations in SEE and SWE. In all regions, the precipi-
 295 tation is significantly correlated with at least one of the two MSLP indices, and
 296 in three regions the precipitation is significantly correlated with both indices.

297 A multiple linear regression model for the estimated precipitation, $P_{\text{lin}i}$, in
 298 each region i is constructed using MSLP_{UK} and MSLP_{NSI} as predictors. Thus
 299 for region i :

$$P_{\text{lin}i} = \alpha_i \text{MSLP}_{\text{UK}} + \beta_i \text{MSLP}_{\text{NSI}} + c_i. \quad (1)$$

300 Each region i has a different set of regression coefficients α_i , β_i and c_i which
 301 represent the relative importance of MSLP_{UK} and MSLP_{NSI} as atmospheric
 302 drivers of precipitation in that region. The forward selection stepwise linear re-
 303 gression method is used. A significance criterion of $p < 0.1$ is used for inclusion
 304 in the regression model: if $p > 0.1$ for one of the MSLP indices then the corre-
 305 sponding regression coefficient is 0. The regression coefficients for each region
 306 are shown in Table 2. Here the standardised MSLP indices are used; that is,
 307 anomalies are computed which are normalised by the standard deviation of the
 308 index over the training period. $P_{\text{lin}i}$ is therefore an estimate of the standard-
 309 ised precipitation anomaly, which can be scaled by the standard deviation of
 310 the observed precipitation timeseries for each region, and recentred about the
 311 mean, to give an actual precipitation estimate. Since the coefficients are for the
 312 precipitation anomaly, the term $c_i = 0$. For correlation scores this choice of
 313 standardisation makes no difference. The impact of detrending the MSLP_{NSI} ,
 314 MSLP_{UK} and precipitation timeseries was found to make almost no difference
 315 to the results (correlations within 0.01), so the non-detrended values are used.

316 For each region the correlation between $P_{\text{lin}i}$ and the observed precipitation
 317 is shown in Fig. 5a (purple bars). To evaluate the derived precipitation against
 318 observed precipitation, the Spearman rank correlation is used in preference to
 319 the Pearson correlation, as this avoids making assumptions about linearity, and
 320 deals better with outliers (Wilks, 1995). Using the Pearson correlation gives
 321 generally similar results. The correlations between $P_{\text{lin}i}$ and observed precip-
 322 itation are significant in all regions. The highest correlations are in SEE and
 323 SWE, with the lowest correlations in ES and NEE. In all regions apart from ES
 324 and NEE, this method explains more than 50% of the precipitation variance (i.e.
 325 the correlation $r \geq 0.71$), while in SEE more than 75% of variance is explained
 326 ($r \geq 0.87$). Fig. 6c shows that the highest correlations are obtained for regions
 327 in the north-west and south of the country, with north-eastern regions having
 328 the lowest correlations.

329 To evaluate the simple multiple linear regression model, the coefficients de-
 330 rived for the 1931–1991 training period were applied to observed MSLP data for
 331 the test period 1992–2011, and the results evaluated against regional precipita-
 332 tion for this later period. Timeseries of the observed and derived precipitation
 333 for three sample regions are shown in Fig. 7. In NS (Fig. 7a) there is very
 334 good agreement between observed and derived precipitation, and in particu-
 335 lar the precipitation extremes are well captured. In NWE (Fig. 7b), where
 336 precipitation is controlled by both pressure indices relatively equally, the ex-
 337 tremes are again well captured, but there are a few years where the derived
 338 precipitation does not match the observed precipitation. A similarly good cor-
 339 respondence between observed and derived precipitation is seen for CE (Fig.
 340 7c), but again there are a few years where the derived precipitation does not
 341 match the observed. The years with poor correspondence between derived and

342 observed precipitation tend to be those where the precipitation is close to the
343 mean value, which suggests that the model may not perform so well when the
344 driving circulation patterns are weak. The correlations for the test period are
345 shown in Fig. 5b. These are similar to the correlations for the training period
346 (Fig. 5a). The good agreement between the downscaled and observed precip-
347 itation for the independent evaluation period suggest that the multiple linear
348 regression model is robust, and is not over-fitted to the training dataset. Repeat-
349 ing the evaluation of the multiple regression model on other 20-year sub-periods
350 (1932–1951, 1952–1971 and 1972–1991) also give similar correlations to those
351 for the full training period. In regions NI and NWE, there is a difference in
352 the relative importance of the two pressure indices between the training period
353 and the test period: in the training period precipitation in these regions has a
354 higher correlation with $MSLP_{UK}$ than $MSLP_{NSI}$, while in the test period the
355 correlation with $MSLP_{NSI}$ is higher (compare Fig. 5a and b). This emphasizes
356 the need for a long training period that is independent from the test period.

357 The same methodology can be applied to the UKCP09 gridded precipitation
358 data. A multiple linear regression model based on the two pressure indices
359 can be derived for each grid point, over the training period 1931–1991. As
360 for the regional precipitation, this leads to the strongest correlations between
361 observed and derived precipitation in the south of England and the north-west
362 of Scotland, with slightly lower correlations in the north-east of the country (not
363 shown). The observed MSLP-precipitation relationships derived for each grid
364 point are used in Section 5.2 to derive forecasts of precipitation on these scales.

365 5 Seasonal precipitation forecasts using the mul- 366 tiple linear regression model

367 The aim of this section is to evaluate seasonal hindcasts of UK regional precip-
368 itation obtained by applying the multiple linear regression model developed in
369 Section 4 to GloSea5 hindcasts of MSLP.

370 5.1 Evaluation of GloSea5

371 The current GloSea5 system has been shown to have good skill in forecasting
372 the wintertime NAO from forecasts initialised around the start of November,
373 with a correlation skill score of 0.62 for the period 1992–2011 (Scaife *et al.*,
374 2014). Less has been said about the skill in forecasting precipitation, although
375 MacLachlan *et al.* (2015) showed that there was little skill in raw model output
376 for Northern Europe for DJF upper and lower terciles of precipitation (their
377 Figure 13). Figure 8(a) shows a map of the correlation skill for the ensemble
378 mean precipitation from GloSea5 evaluated against the UKCP09 gridded pre-
379 cipitation observations (regridded first to the GloSea5 grid). There are a few
380 gridboxes with high skill (correlations exceeding 0.5), mostly in south Wales
381 and moderate (but not significant) skill in some gridboxes in western Scotland.
382 In general the grid-point skill within the HadUKP regions is coherent, although
383 in the SWE region this is not true, as South Wales has higher skill than further
384 south. Most of the eastern parts of the UK have low or no skill (correlations less
385 than 0 in some places). These results should, however be taken with caution

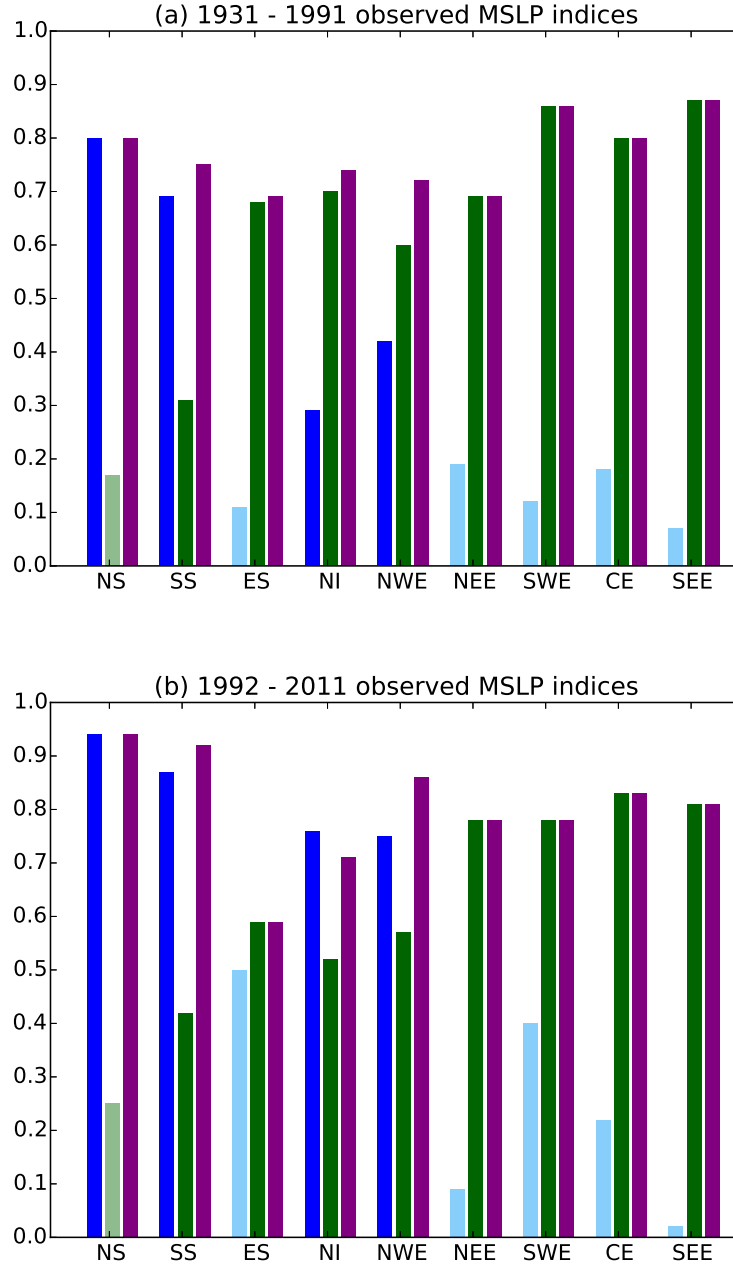


Figure 5: Absolute value of Spearman rank correlations between observed winter regional precipitation and the two pressure indices $MSLP_{NSI}$ (blue), $MSLP_{UK}$ (green) and derived precipitation P_{lin} (purple) for (a) the training period (1931–1991) and (b) the test period (1992–2011). Correlations that are not significant ($p > 0.1$) in the training period (and therefore correspond to indices not used in the construction of P_{lin}) are shown in pale blue/green.

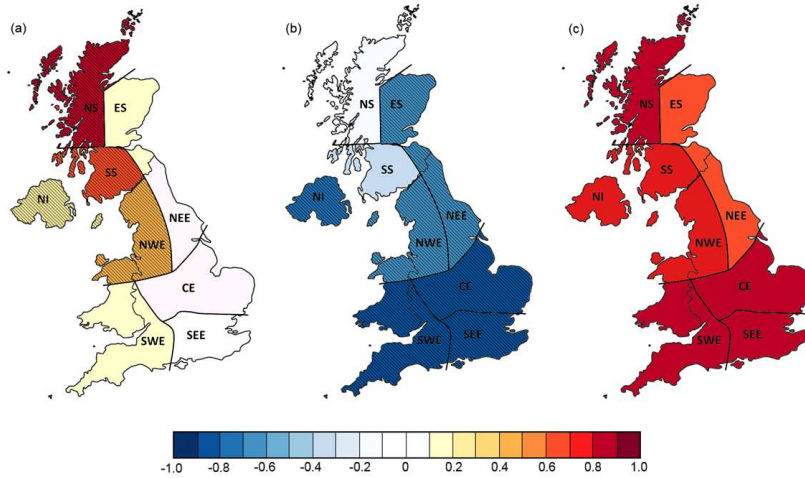


Figure 6: Correlation between winter regional precipitation and (a) $MSLP_{NSI}$, (b) $MSLP_{UK}$, and (c) P_{in} for observations in the training period (1931–1991). In (a,b) correlations that are significant at the 90% level are overlaid with hatched lines; in (c) all correlations are significant so hatching is omitted for clarity.

386 since data output from models such as seasonal forecast models is not designed
 387 to be evaluated on the grid-point scale (e.g. Lander and Hoskins, 1997).

388 Figure 9 shows a spatial map of the skill of the GloSea5 ensemble mean in directly
 389 forecasting DJF MSLP, as compared to the HadSLP2 observation dataset, over a domain
 390 covering the North Atlantic and Europe. Regions over the UK and to the north and south,
 391 including the $MSLP_{NSI}$ centres, have reasonable skill, with correlation values between
 392 0.4 and 0.6. The model correlation skill scores for the two indices defined in Section 4
 393 are 0.56 for $MSLP_{NSI}$, and 0.50 for $MSLP_{UK}$. These are both significant at the 95%
 394 level. The skill of GloSea5 in forecasting DJF atmospheric circulation variability in the
 395 North Atlantic is therefore not restricted to the NAO, but also includes other modes of
 396 variability.

397 It is also important to understand whether the GloSea5 forecast system
 398 can spatially represent the atmospheric drivers of UK regional precipitation. Correlation
 399 maps of MSLP against $MSLP_{NSI}$ and $MSLP_{UK}$ are shown in Fig. 10, both for the
 400 observations for the full period 1931–2011 and for GloSea5 for the period 1992–2011.
 401 As expected, the observed correlation pattern for $MSLP_{NSI}$ (Fig. 10a) shows a dipole
 402 structure, and looks almost identical to the NS precipitation correlation pattern (Fig. 3a).
 403 The equivalent correlation map for GloSea5 is very similar (Fig. 3b), although the
 404 southern centre of the dipole is slightly weaker in GloSea5 than the observations. The
 405 observed correlation pattern for $MSLP_{UK}$ (Fig. 10c) looks much like the SEE
 406 correlation pattern (Fig. 3i) with the signs reversed. The equivalent correlation map
 407 for GloSea5 again strongly resembles the observed pattern (Fig. 10d). The fact that
 408 these correlation maps are similar for GloSea5 and for the observations indicates that
 409 these MSLP indices correspond to the same atmospheric circulation patterns.
 410

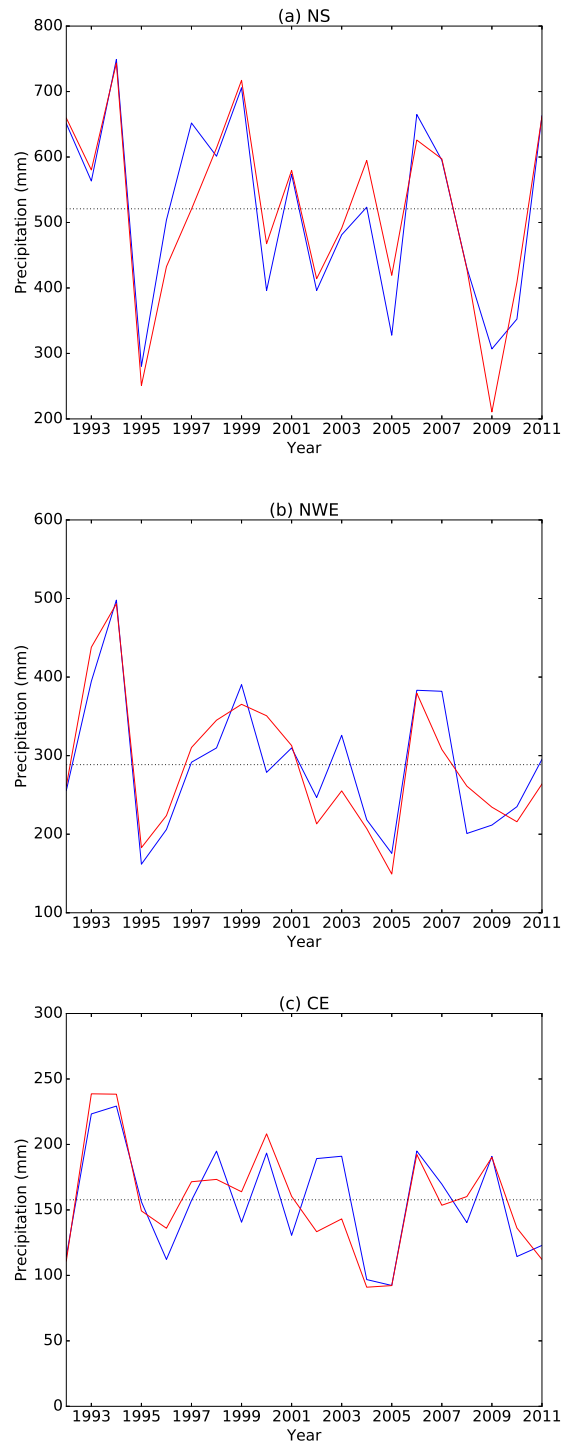


Figure 7: Time series of DJF observed precipitation (blue lines) and precipitation derived using the multiple linear regression model applied to HadSLP2 observed pressure indices (red lines), for the period 1992–2011. Panels show precipitation in (a) Northern Scotland, (b) North-West England and (c) Central England. The dotted black line marks the time-mean observed precipitation.

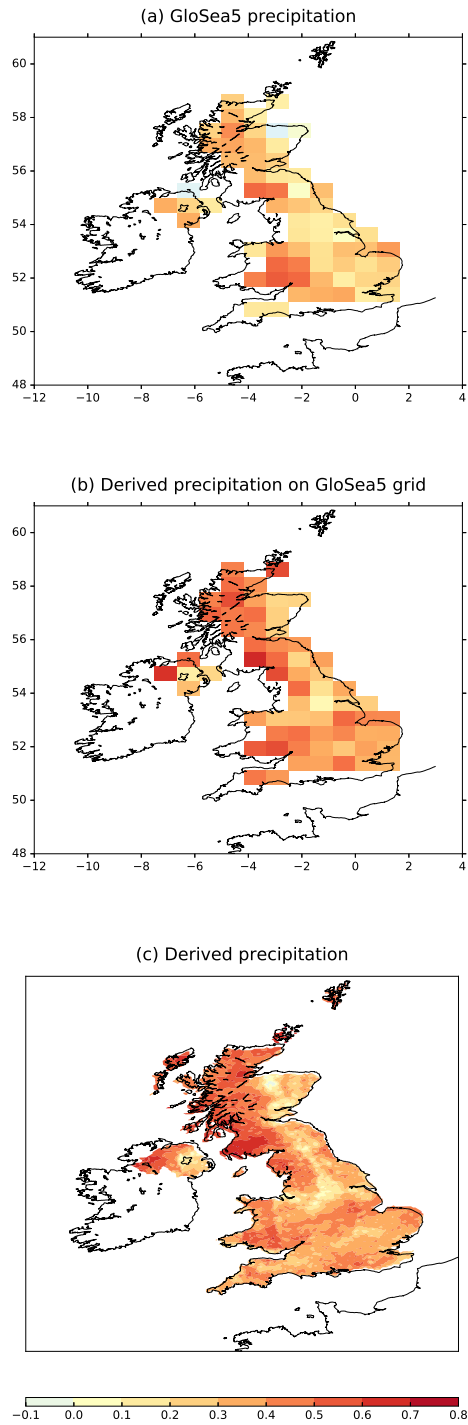


Figure 8: Spearman rank correlation scores for winter precipitation for the period 1992–2011. (a) Correlation skill for ensemble mean precipitation from GloSea5 at each grid-box compared with the UKCP09 observed precipitation regridded to the GloSea5 model grid. (b,c) Correlation skill for ensemble mean precipitation derived from GloSea5 MSLP indices using the multiple linear regression model compared with the UKCP09 observed precipitation. In (b) the correlation map is regridded to the GloSea5 grid for comparison with (a); (c) is on the native UKCP09 5km grid.

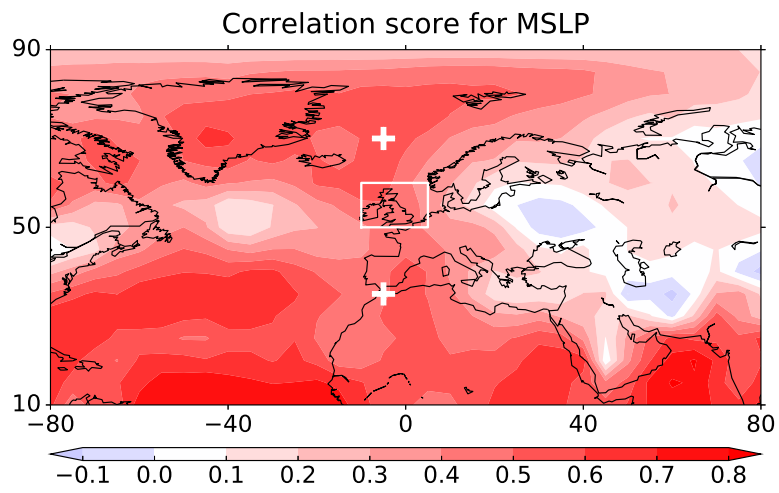


Figure 9: Correlation skill score between GloSea5 ensemble mean MSLP and observed MSLP for the hindcast period 1992–2011. ‘+’ symbols indicate the locations of the MSLP_{NSI} centres, while the rectangular box indicates the averaging area for MSLP_{UK} .

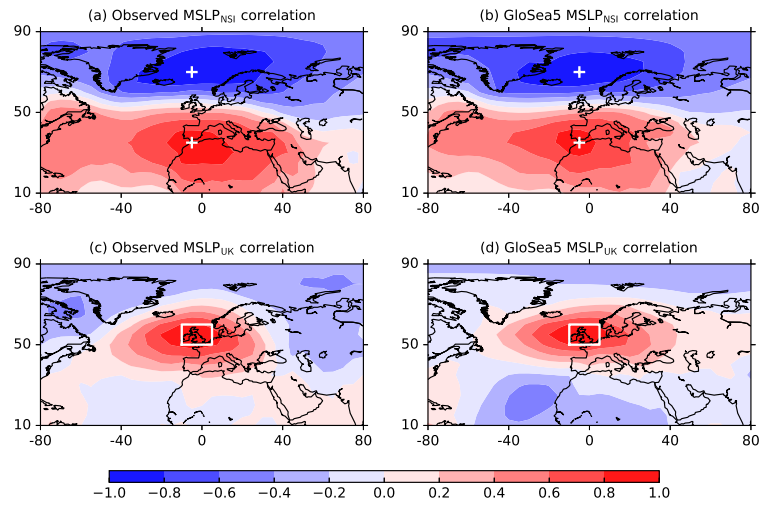


Figure 10: Point-based correlation between MSLP fields and (a, b) MSLP_{NSI} and (c, d) UK MSLP, for (a, c) observations for the period 1931–2011 and (b, d) GloSea5 for the period 1992–2011. In (b,d) the map shows the mean of the individual ensemble members' correlations between MSLP and the respective indices. '+' symbols in (a,b) indicate the MSLP_{NSI} centres, while the rectangle in (c,d) indicates the averaging area for MSLP_{UK} .

411 5.2 Forecasting precipitation using the multiple linear re- 412 gression model based on observations

413 The multiple linear regression model was applied to the GloSea5 hindcasts of
414 the two pressure indices. The model was applied to each ensemble member
415 individually. In this section the skill for the ensemble mean is discussed. In Sec-
416 tion 5.3 a discussion of how this method can be used to produce a probabilistic
417 forecast is given.

418 Figure 11 shows the skill obtained in forecasting precipitation for each re-
419 gion by applying the multiple linear regression model to the $MSLP_{NSI}$ and
420 $MSLP_{UK}$ indices obtained from the GloSea5 hindcast data for DJF, from fore-
421 casts initialised around the start of November. The highest skill is obtained
422 for NS, which has a correlation skill score of 0.64. CE and SS also have high
423 correlation scores above 0.5. NI and NWE have reasonable correlation scores
424 above 0.4, which are significant at the 90% level. The remaining three regions
425 have lower skill, with the lowest correlation skill score seen in SWE.

426 The high skill in forecasting NS and SS precipitation is due to the model's
427 relatively high skill in forecasting the $MSLP_{NSI}$, and the high correlation be-
428 tween this pressure index and precipitation in these regions (Fig. 12). The fact
429 that good skill is obtained in the north-west of the UK is consistent with the
430 findings of Svensson *et al.* (2015) that this region is strongly influenced by the
431 NAO, which is a similar MSLP dipole index to $MSLP_{NSI}$.

432 In regions NI and NWE, significant skill in forecasting precipitation is also
433 obtained (Fig. 11). It can be seen from Fig. 12, however, that in these regions,
434 the correlation between GloSea5 forecast $MSLP_{NSI}$ and observed precipitation
435 is higher than the correlation between the estimated precipitation P_{lin} and ob-
436 served precipitation. This is related to the fact that, in these two regions, in
437 the test period the observed precipitation is more strongly related to observed
438 $MSLP_{NSI}$ while in the training period $MSLP_{UK}$ is more important (as dis-
439 cussed at the end of Section 4). For more general periods it would therefore
440 be advisable to use P_{lin} rather than only $MSLP_{NSI}$ to forecast precipitation in
441 these regions.

442 The remaining regions are those where precipitation is driven by $MSLP_{UK}$.
443 CE has relatively high skill (0.51) compared to the remaining four regions. ES
444 and NEE are the two regions with the lowest correlations in the observations in
445 the training period, so this is not unexpected. In contrast, SEE and SWE have
446 relatively low correlation skill scores, but have the highest correlations in the ob-
447 servations between the actual precipitation and predicted precipitation P_{lin} , and
448 therefore high potential predictability. This is partly due to the lower skill in the
449 model forecast of $MSLP_{UK}$ compared with the skill for $MSLP_{NSI}$. Therefore
450 future improvements in GloSea5's ability to represent variability in $MSLP_{UK}$
451 would lead to improvements in precipitation forecasts using this method.

452 Using relationships derived for the UKCP09 gridded precipitation data, it
453 is possible to apply this methodology to generate high-resolution gridded pre-
454 cipitation forecasts. Figure 8c shows the correlation scores obtained using this
455 method to forecast precipitation at each grid point in the UK. This shows a
456 similar pattern of skill to that for regional precipitation, with the highest skill
457 seen in the north-west of the UK. In this case Southern Scotland has areas with
458 the highest correlation skill. There are some differences in detail; in particular
459 there is a narrow band of regions with lower skill extending southwards from

460 north-east Scotland; this is collocated with high orography, and may be a result
 461 of limited or less reliable observations in these regions. These results are also
 462 shown regridded to the GloSea5 grid in Fig. 8b, for comparison with the GloSea5
 463 direct precipitation output. This downscaling method gives an improvement in
 464 skill over the GloSea5 direct precipitation output in most gridboxes. There are
 465 a few gridboxes, in Northern Ireland and the West of England where the derived
 466 precipitation gives slightly worse results than GloSea5 direct precipitation out-
 467 put. However, it should be noted that the 5km precipitation forecast obtained
 468 using this method are potentially much more useful for streamflow modelling, as
 469 it will allow distinction between river basins not possible with the much coarser
 470 resolution GloSea5 precipitation forecast.

471 5.3 Generating a probabilistic forecast for regional pre- 472 cipitation

473 We have focussed on correlation skill so far because unlike probabilistic mea-
 474 sures like reliability, the correlation is robust to post-processing changes to the
 475 ensemble spread. Nevertheless, probabilistic forecasts are useful to represent
 476 uncertainty and so in this section we demonstrate how a well calibrated prob-
 477 abilistic forecast for UK regional precipitation can be produced. *Scaife et al.*
 478 (2014) noted that, while the winter NAO prediction skill is high, the magni-
 479 tude of the signal in the ensemble mean is much smaller than the interannual
 480 variability of the observations. Furthermore, the forecast skill is higher than
 481 would be expected given the size of the ensemble mean signal and the ensem-
 482 ble spread. To address this issue, *Eade et al. (2014)* defined a quantity, which
 483 they termed the ratio of predictable components (RPC), to give an estimate
 484 of the ratio of the ‘predictability of the real world’ to the ‘predictability of
 485 the model’. The ‘predictability of the real world’ is estimated by the ensem-
 486 ble mean correlation coefficient with the observations, while the ‘predictability
 487 of the model’ is estimated from the standard deviation of the ensemble mean
 488 divided by the standard deviation of ensemble members. This quantity should
 489 be 1 for a perfect forecast system. *Eade et al. (2014)* developed a method to
 490 correct the ensemble mean signal and ensemble members accordingly, to make
 491 RPC equal to unity. This method alters the ensemble mean variance according
 492 to the correlation skill, and adjusts the ensemble members such that the ensem-
 493 ble variance about the ensemble mean is equal to the unpredictable noise of the
 494 observations. The correction does not affect correlation skill and is described
 495 in full in *Eade et al. (2014)*. The correction method can be applied in real-time
 496 using ensemble information from a hindcast period. The RPC and the correc-
 497 tion method are described in more detail in Appendix B. Here we show results
 498 both with and without this correction by applying it to the GloSea5 predictions
 499 of MSLP_{NSI} and MSLP_{UK} before they are used to infer rainfall. The RPC
 500 values for MSLP_{NSI} and MSLP_{UK} are 2.07 and 1.48, respectively.

501 The observed and estimated precipitation timeseries for two regions (NS and
 502 CE) obtained for the 20-year test period are shown in Figure 13. Although the
 503 correlation skill is high for NS precipitation (0.64, Fig. 11), Fig. 13a shows that
 504 the magnitude of the signal in the ensemble mean predicted precipitation is much
 505 smaller than that of the observed precipitation variability, by a factor of 5. The
 506 ensemble is also overdispersed; the ensemble spread is larger than the observed
 507 extreme precipitation values in the timeseries. Similarly the magnitude of the

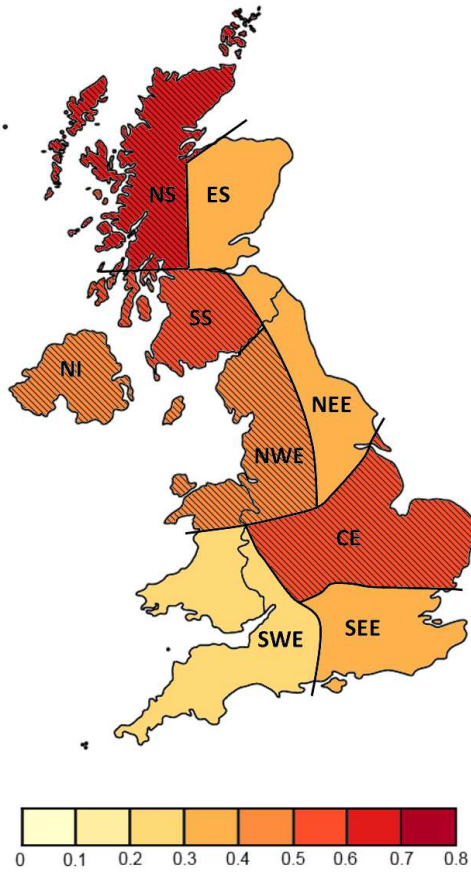


Figure 11: Spearman rank correlation skill for predicting winter precipitation in each of the HadUKP regions using the multiple linear regression model applied to GloSea5 MSLP fields for the period 1992–2011. Correlations that are significant at the 90% level are overlaid with hatched lines.

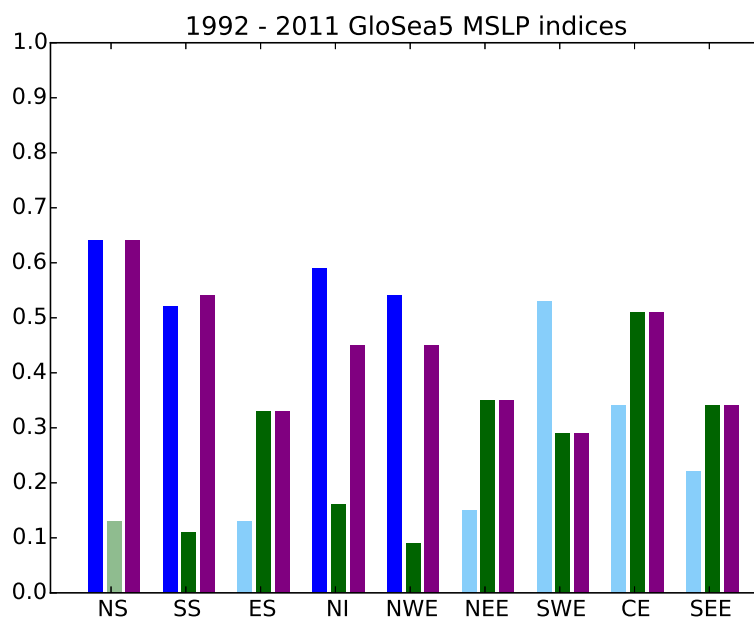


Figure 12: Absolute value of Spearman rank correlations between observed winter regional precipitation and the two pressure indices $MSLP_{NSI}$ (blue), $MSLP_{UK}$ (green) and derived precipitation P_{in} (purple) from GloSea5 hindcasts, over the period 1992–2011. Correlations that are not significant ($p > 0.1$) in the training period (and therefore correspond to indices not used in the construction of P_{in}) are shown in pale blue/green.

508 signal of the CE ensemble mean precipitation estimates (Fig. 13b) is a factor
509 of 3 smaller than the observed precipitation variability in this region, and the
510 ensemble spread is again large. Similar features are also seen for precipitation in
511 the remaining seven regions (not shown). Equivalent series produced using the
512 RPC-corrected pressure indices are shown in Figures 13c and d. For NS (Fig.
513 13c) using the RPC correction gives an ensemble mean signal magnitude around
514 double that obtained using the uncorrected values (Fig. 13a). The ensemble
515 spread is also smaller in this case. In particular, in winters 1994 and 2011, the
516 ensemble forecast confidently predicts the high precipitation anomalies observed.
517 The RPC correction has less effect on CE precipitation predictions (Fig. 13d)
518 and other regions where precipitation is driven mainly by MSLP_{UK} . This is
519 due to the lower correlation skill for MSLP_{UK} , which means that the inflation
520 of the ensemble mean signal is smaller. Nevertheless, the ensemble mean signal
521 for CE precipitation is increased by a factor of 1.5 by the RPC correction, and
522 gives smaller ensemble variance than obtained using the uncorrected values (Fig.
523 13b). Finally, it is interesting to note that in winter 2011, both the observations
524 and ensemble mean show a relatively large positive precipitation anomaly in NS
525 (Figs. 13a and c) and a relatively large negative precipitation anomaly in CE
526 (Figs. 13b and d). This is an example of how this method can predict regional
527 differences in precipitation.

528 To give a probabilistic evaluation of the ensemble forecasts' ability to predict
529 higher or lower than average precipitation, the Brier skill score is used (see
530 Appendix A for more details). Brier skill scores for each region are shown in
531 Table 3, for both the uncorrected and RPC-corrected ensembles. In all regions
532 except for ES the BSS is greater than zero, indicating that the ensemble forecast
533 has more skill than climatology. In general the RPC-corrected ensemble gives
534 better Brier skill scores than the uncorrected ensemble. However, in the regions
535 with low skill (ES and SWE) the RPC correction does not improve the Brier
536 skill scores. The five regions with significant correlation skill (Fig. 11) have
537 high Brier skill scores, while those with lowest correlation skill have lower Brier
538 skill scores.

539 6 Discussion and conclusions

540 The aim of this study was to determine whether skilful seasonal forecasts of the
541 large-scale atmospheric circulation can be downscaled to provide skilful seasonal
542 forecasts of UK regional precipitation.

543 Precipitation in the UK has a north-west/south-east gradient, in terms of
544 both the total amount of precipitation and the main atmospheric drivers of pre-
545 cipitation. This gradient is stronger in winter than in summer. In winter, there
546 are two distinct atmospheric circulation patterns associated with precipitation
547 variability in the north-west regions and in the south-east regions. Precipita-
548 tion in the north-west is associated with a MSLP dipole with centres to the
549 north and south of the UK (which we refer to as the MSLP_{NSI} index); precip-
550 itation in the south-east is associated with a MSLP anomaly centred over the
551 UK (which we refer to as the MSLP_{UK} index). These modes of variability re-
552 semble eastward-shifted versions of the NAO and the EA Pattern, respectively.
553 GloSea5 seasonal hindcasts were found to skilfully represent both these modes
554 of variability in winter in forecasts initialised around the start of November.

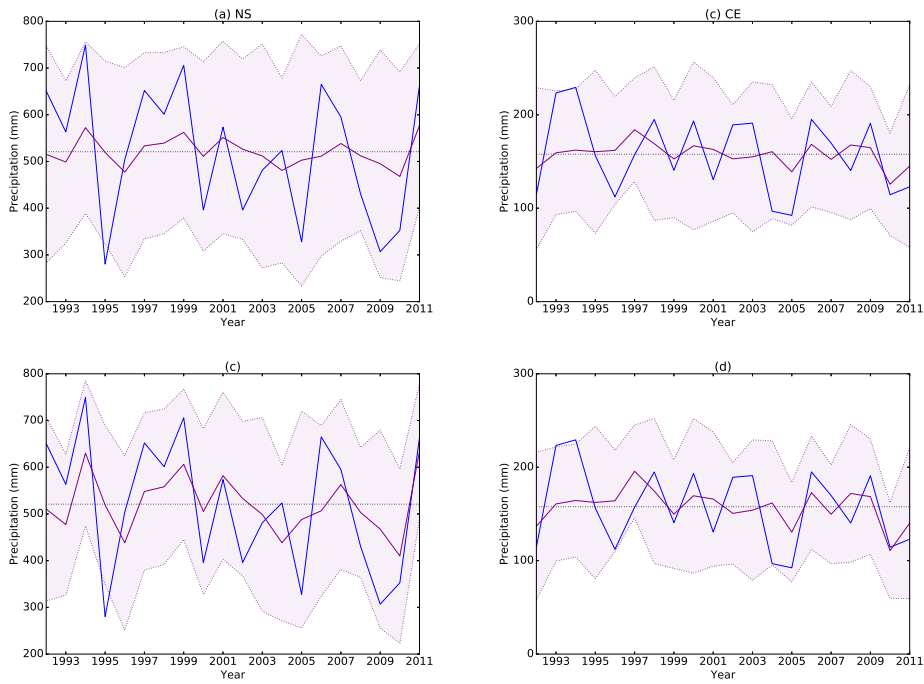


Figure 13: Timeseries of observed and estimated winter precipitation (in mm) in regions (a,c) Northern Scotland and (b,d) Central England. Blue lines show the observed precipitation, purple lines show the ensemble mean estimate precipitation, with shading and dotted purple lines indicating plus and minus two standard deviations of the ensemble member estimates. The dotted black line marks the time-mean observed precipitation. (a) and (b) show timeseries obtained using the unadjusted ensemble forecasts of $MSLP_{NSI}$ and $MSLP_{UK}$; (c) and (d) show timeseries obtained using the RPC-corrected ensemble forecasts of $MSLP_{NSI}$ and $MSLP_{UK}$.

555 The skill of GloSea5 in winter is therefore not restricted to the NAO, but also
556 extends to MSLP variability centred over the UK.

557 A simple multiple linear regression model has been developed to describe
558 the variability of winter precipitation in each UK region, using indices based
559 on these two circulation patterns. This multiple linear regression model de-
560 scribes between 50 and 76% of observed precipitation variability in each region.
561 Applying this multiple linear regression model to GloSea5 seasonal hindcasts
562 of winter MSLP leads to more skilful forecasts than simply using precipitation
563 forecasts directly from GloSea5. The correlation skill is particularly high for
564 north-western regions of the UK (0.64), in which precipitation is driven primar-
565 ily by the MSLP_{NSI} dipole-based index. In general lower skill is obtained for
566 south-eastern regions, which are more strongly influenced by the MSLP_{UK} in-
567 dex, although Central England shows promising forecast correlation skill (0.51).
568 The generally lower skill in England than in Scotland may be because GloSea5
569 has lower skill for MSLP_{UK} than for MSLP_{NSI} , therefore improvements in
570 forecasting MSLP over the UK could lead to skilful seasonal forecasts of winter
571 precipitation for all UK regions.

572 The downscaling methodology developed in this study has also be applied
573 to the UKCP09 5km gridded precipitation data, which gives broadly similar
574 results to the regional analysis. Comparison between the derived precipitation
575 and GloSea5 direct precipitation output showed that this downscaling technique
576 gives better correlation skill than simply using the direct GloSea5 precipitation
577 output. In addition, the 5km gridded precipitation forecast produced using this
578 method are potentially useful for streamflow modelling, as they allow distinction
579 between river basins not possible with the much coarser resolution GloSea5
580 precipitation forecasts. Due to the constraints of computational cost, seasonal
581 forecast models cannot currently be run at higher resolution, and certainly they
582 will not be run operationally at horizontal resolutions close to 5km in the near
583 future. Even if run at kilometre-scale resolutions, biases in the model mean state
584 such as positioning of the North Atlantic jet would make it difficult to use direct
585 precipitation output from these models on seasonal timescales, so downscaling
586 methods such as the one used in this paper would still be useful.

587 A probabilistic ensemble forecast for regional UK precipitation can be made
588 using this methodology by applying the multiple linear regression model to
589 MSLP_{UK} than for MSLP_{NSI} forecast by individual GloSea5 ensemble member.
590 However, post-processing of the ensemble forecasts must be performed in order
591 to correct for the low signal-to-noise ratio of the ensemble. The RPC correction
592 used here is one such post-processing technique. Applying this correction to
593 the forecast pressure indices gives a larger signal in the ensemble mean regional
594 precipitation forecasts, and smaller ensemble spread, or more confident forecasts.
595 Brier skill scores show that the ensemble of derived precipitation forecasts using
596 this method has skill higher than climatology in most regions.

597 This multiple linear regression approach could also be applicable to decadal
598 forecasting and future climate projections. In these lower-resolution models,
599 regions with different precipitation drivers could well be contained within one
600 gridbox. The sub-grid-scale or near-grid-scale variability means that it is dif-
601 ficult to use precipitation directly from these models to provide forecasts or
602 to draw conclusions about future changes in precipitation. In particular, the
603 larger interannual variability of precipitation received by north-western UK re-
604 gions compared to those in the south-east means that variability in precipitation

605 in the north-western regions dominate variability in the UK total precipitation.
606 As shown in this study, precipitation in the south-east and north-west regions is
607 uncorrelated. Therefore any forecast or projection based on a UK-average pre-
608 cipitation contains little information about precipitation in south-eastern UK
609 regions. This has implications for forecasts or future projections of drought,
610 to which the south-east is more vulnerable than the north-west (Folland *et al.*,
611 2015). Using the multiple linear regression model, however, provides informa-
612 tion about each region separately. One consideration for using this method in
613 this context would be how much the relationship between atmospheric circula-
614 tion and regional precipitation can be assumed to be stationary over longer
615 timescales.

616 The method used in this study was designed to utilise known skill of the
617 GloSea5 model at forecasting the wintertime NAO and circulation described by
618 MSLP. If other fields such as vorticity, wind strength and wind direction can
619 be forecast with similar levels of skill, then a similar method could be devel-
620 oped based on the Jenkinson indices (Jenkinson and Collison, 1977), utilising
621 the relationships between these and regional precipitation found by Jones *et al.*
622 (2014). Future model developments will lead to further increases in forecasting
623 skill for atmospheric circulation patterns, both due to higher model resolution
624 and larger ensemble sizes. This increased skill could be utilised in more complex
625 downscaling methods, perhaps using the above-mentioned fields in addition to
626 MSLP. In addition, furthering our understanding of the processes that underlie
627 modes of atmospheric variability such as the NAO is essential for improving
628 seasonal predictions and capturing the relationships with patterns of precip-
629 itation. This includes external processes such as ocean-atmosphere coupling
630 (e.g. Kushnir, 1994) and internal atmospheric processes such as eddy-mean flow
631 interactions (e.g. Wallace and Lau, 1985).

632 This study has focused on winter only for building the multiple linear regres-
633 sion model. However a similar approach can also be used for summer. Based on
634 the correlation patterns in Fig. 4, two MSLP indices can be identified to model
635 regional summer precipitation variability: the first index is a representation
636 of the SNAO, defined using the pressure difference between a Greenland box
637 (70°W – 45°W , 70°N – 85°N) and a UK box (defined as for winter); the second
638 index is the pressure at (5°W , 60°N). Constructing a multiple linear regression
639 model with observations of these two indices gives correlations with observed re-
640 gional summer precipitation of between 0.7 and 0.8, so this model explains more
641 than about 50% of the precipitation variability in each region. In future sea-
642 sonal forecast models with more skilful representation of summer atmospheric
643 circulation, this method could be useful in forecasting summer precipitation as
644 well as winter.

645 Acknowledgements

646 LHB was supported by the NERC project IMPETUS (ref. NE/L010488/1).
647 AAS was supported by the Joint DECC/Defra Met Office Hadley Centre Cli-
648 mate Programme (GA01101). We thank the two anonymous reviewers for pro-
649 viding helpful comments and suggestions on the manuscript.

650 A The Brier skill score

651 In Section 5.3 the Brier skill score is used to evaluate the probabilistic skill of the
 652 forecasts at forecasting higher or lower than average precipitation. Following
 653 (Jolliffe and Stephenson, 2003), the Brier skill score is defined as

$$\text{BSS} = 1 - \frac{B}{B_{\text{ref}}}, \quad (2)$$

654 where B is Brier score B , defined as

$$B = \frac{1}{n} \sum_{j=1}^n f_j - o_j, \quad (3)$$

655 n is the number of years, f_j is the forecast probability of the event in year
 656 j , and o_j is equal to 1 if the event occurred and 0 if not. In this case the
 657 event is the occurrence of higher (or lower) than average precipitation in a
 658 given region. The forecast probability f_j is calculated by taking the average of
 659 all ensemble members' forecasts of the event occurring (either 1 or 0 for each
 660 ensemble member). B_{ref} is the climatology, in this case 0.5 since higher (lower)
 661 than average precipitation occurs 50% of the time.

662 Brier skill score values greater than 0 indicate that the ensemble system is
 663 more skilful than climatology; negative values indicate poorer skill than clima-
 664 tology.

665 B The ratio of predictable components (RPC) 666 and RPC correction

667 In Section 5.3 the RPC correction is used. The RPC gives an estimate of the
 668 ratio of the 'predictability of the real world' to the 'predictability of the model'
 669 (Eade *et al.*, 2014). The predictable component of the observations (PC_{obs}) is
 670 defined as the correlation r between the ensemble mean and observations, given
 671 by

$$\text{PC}_{\text{obs}} = r = \frac{\sum_{j=1}^n (\bar{x}_j - \hat{x})(y_j - \hat{y})}{\sqrt{\sum_{j=1}^n (\bar{x}_j - \hat{x})^2 \sum_{j=1}^n (y_j - \hat{y})^2}}, \quad (4)$$

672 where \bar{x}_j and y_j are the ensemble mean and observation (respectively) in year j ,
 673 and \hat{x} and \hat{y} are the time-means of these quantities over n years. The predictable
 674 component of the model (PC_{mod}) is defined as the ratio of the ensemble mean
 675 standard deviation to the average ensemble member standard deviation, given
 676 by

$$\text{PC}_{\text{mod}} = \sqrt{\frac{\sigma_{\bar{x}}^2}{\frac{1}{m} \sum_{i=1}^m \sigma_{x_i}^2}}, \quad (5)$$

677 where m is the number of ensemble members, x_i is ensemble member i and σ_x
 678 represents the standard deviation over time of a quantity x . The RPC is then
 679 defined as the ratio

$$\text{RPC} = \frac{\text{PC}_{\text{obs}}}{\text{PC}_{\text{mod}}}. \quad (6)$$

680 RPC can have any value, but if the model predictability accurately reflects the
 681 observed predictability then $\text{RPC}=1$. Values of RPC greater than one indicate
 682 an overdispersive system; positive values lower than one indicate underdispers-
 683 sion; and negative values indicate that there is no skill.

684 The RPC correction developed by Eade *et al.* (2014) adjusts the ensemble
 685 mean and ensemble members such that the $\text{RPC}=1$. The ensemble mean is
 686 adjusted so that its variance is equal to the predictable part of the observed
 687 variance: $\text{PC}_{\text{obs}}^2 = r^2\sigma_y^2$. The adjusted ensemble mean \bar{x}_j' in year j is given by

$$\bar{x}_j' = (\bar{x}_j - \hat{x}) \frac{\sigma_y r}{\sigma_x} + \hat{x}, \quad (7)$$

688 where σ_y is the standard deviation of the observations. The ensemble members
 689 are then recentred about the adjusted mean and their variance adjusted to
 690 be equal to the variance of the unpredictable noise part of the observations:
 691 $(1 - r^2)\sigma_y^2$. The adjusted ensemble member i at time j , x'_{ij} , is given by

$$x'_{ij} = (x_{ij} - \hat{x}) \frac{\sigma_y \sqrt{(1 - r^2)}}{\sigma_{\text{mem}j}} + \bar{x}_j' \quad (8)$$

692 where $\sigma_{\text{mem}j}$ is the standard deviation of the ensemble members about the
 693 ensemble mean at time j . Full details can be found in Eade *et al.* (2014).

694 References

- 695 Alexander L, Jones P. 2000. Updated precipitation series for the UK and dis-
 696 cussion of recent extremes. *Atmos. Sci. Let.* **1**(2): 142–150, doi:10.1006/asle.
 697 2000.0016.
- 698 Allan R, Ansell T. 2006. A new globally complete monthly historical gridded
 699 mean sea level pressure dataset (hadslp2): 1850-2004. *Journal of Climate*
 700 **19**(22): 5816–5842, doi:10.1175/JCLI3937.1.
- 701 Barnston AG, Livezey RE. 1987. Classification, seasonality and persistence
 702 of low-frequency atmospheric circulation patterns. *Mon. Weather Rev.* **115**:
 703 1083–1126.
- 704 Eade R, Smith D, Scaife A, Wallace E, Dunstone N, Hermanson L, Robinson
 705 N. 2014. Do seasonal-to-decadal climate predictions underestimate the pre-
 706 dictability of the real world? *Geophysical research letters* **41**(15): 5620–5628,
 707 doi:10.1002/2014GL061146.
- 708 Folland C, Hannaford J, Bloomfield J, Kendon M, Svensson C, Marchant
 709 B, Prior J, Wallace E. 2015. Multi-annual droughts in the English Low-
 710 lands: a review of their characteristics and climate drivers in the winter
 711 half-year. *Hydrology and Earth System Sciences* **19**(5): 2353–2375, doi:
 712 10.5194/hess-19-2353-2015.
- 713 Folland CK, Knight J, Linderholm HW, Fereday D, Ineson S, Hurrell JW. 2009.
 714 The summer north atlantic oscillation: past, present, and future. *Journal of*
 715 *Climate* **22**(5): 1082–1103, doi:10.1175/2008JCLI2459.1.

- 716 Folland CK, Woodcock A. 1986. Experimental monthly long-range forecasts for
717 the United Kingdom. part I: Description of the forecasting system. *Met. Mag.*
718 **115**: 301–318.
- 719 Fowler H, Ekström M, Kilsby C, Jones P. 2005. New estimates of future changes
720 in extreme rainfall across the uk using regional climate model integrations. 1.
721 assessment of control climate. *Journal of Hydrology* **300**(1): 212–233.
- 722 Gregory J, Jones P, Wigley T. 1991. Precipitation in Britain: an analysis of
723 area-average data updated to 1989. *Int. J. Climatol* **11**(3): 331–345.
- 724 Huntingford C, Marsh T, Scaife AA, Kendon EJ, Hannaford J, Kay AL, Lock-
725 wood M, Prudhomme C, Reynard NS, Parry S, Lowe JA, Screen JA, Ward
726 HC, Roberts M, Stott PA, Bell VA, Bailey M, Jenkins A, Legg T, Otto FEL,
727 Massey N, Schaller N, Slingo J, Allen MR. 2014. Potential influences on the
728 United Kingdom’s floods of winter 2013/14. *Nature Climate Change* **4**(9):
729 769–777, doi:10.1038/nclimate2314.
- 730 Hurrell J, Kushner Y, Ottensen G, Visbeck M. 2003. The North Atlantic oscilla-
731 tion: climatic significance and environmental impact. In: *An overview of the*
732 *North Atlantic oscillation*, Hurrell J (ed), AGU, pp. 1–35.
- 733 Jenkinson A, Collison F. 1977. An initial climatology of gales over the North
734 Sea. *Synoptic Climatology Branch Memorandum* (62). Meteorological Office,
735 Bracknell.
- 736 Jolliffe IT, Stephenson DB. 2003. *Forecast verification*. Wiley. Retrieved 6
737 September 2017, from <http://www.mylibrary.com?ID=27190>.
- 738 Jones PD, Harpham C, Briffa KR. 2013. Lamb weather types derived from
739 reanalysis products. *International Journal of Climatology* **33**(5): 1129–1139,
740 doi:10.1002/joc.3498, URL <http://dx.doi.org/10.1002/joc.3498>.
- 741 Jones PD, Osborn TJ, Harpham C, Briffa KR. 2014. The development of Lamb
742 weather types: from subjective analysis of weather charts to objective ap-
743 proaches using reanalyses. *Weather* **69**(5): 128–132, doi:10.1002/wea.2255,
744 URL <http://dx.doi.org/10.1002/wea.2255>.
- 745 Karpechko AY, Peterson KA, Scaife AA, Vainio J, Gregow H. 2015. Skilful
746 seasonal predictions of Baltic sea ice cover. *Environmental Research Letters*
747 **10**(044007).
- 748 Kendon M, Marsh T, Parry S. 2013. The 2010–2012 drought in England and
749 Wales. *Weather* **68**(4): 88–95.
- 750 Kendon M, McCarthy M. 2015. The UK’s wet and stormy winter of 2013/2014.
751 *Weather* **70**(2): 40–47.
- 752 Kushnir Y. 1994. Interdecadal variations in north atlantic sea surface temper-
753 ature and associated atmospheric conditions. *Journal of Climate* **7**(1): 141–
754 157.

- 755 Lamb HH. 1950. Types and spells of weather around the year in the British
756 Isles : Annual trends, seasonal structure of the year, singularities. *Quarterly*
757 *Journal of the Royal Meteorological Society* **76**(330): 393–429, doi:10.1002/
758 qj.49707633005, URL <http://dx.doi.org/10.1002/qj.49707633005>.
- 759 Lander J, Hoskins B. 1997. Believable scales and parameterizations in a spectral
760 transform model. *Monthly weather review* **125**(2): 292–303.
- 761 Lavers D, Prudhomme C, Hannah DM. 2010. Large-scale climate, precipitation
762 and british river flows: Identifying hydroclimatological connections and dy-
763 namics. *Journal of Hydrology* **395**(3): 242–255, doi:10.1016/j.jhydrol.2010.10.
764 036.
- 765 Lavers D, Prudhomme C, Hannah DM. 2013. European precipitation connec-
766 tions with large-scale mean sea-level pressure (mslp) fields. *Hydrological Sci-*
767 *ences Journal* **58**(2): 310–327, doi:10.1080/02626667.2012.754545.
- 768 MacLachlan C, Arribas A, Peterson K, Maidens A, Fereday D, Scaife A, Gor-
769 don M, Vellinga M, Williams A, Comer R, Camp J, Xavier P, Madec G. 2015.
770 Global seasonal forecast system version 5 (GloSea5): a high-resolution sea-
771 sonal forecast system. *Quarterly Journal of the Royal Meteorological Society*
772 **141**: 1072–1084, doi:10.1002/qj.2396.
- 773 Met Office, Hollis D, McCarthy M. 2017. UKCP09: Met Office gridded and
774 regional land surface climate observation datasets. Centre for Environmental
775 Data Analysis. 15 September 2017.
- 776 Muchan K, Lewis M, Hannaford J, Parry S. 2015. The winter storms of
777 2013/2014 in the UK: hydrological responses and impacts. *Weather* **70**(2):
778 55–61.
- 779 Murphy SJ, Washington R. 2001. United Kingdom and Ireland precipitation
780 variability and the North Atlantic sea-level pressure field. *International Jour-*
781 *nal of Climatology* **21**(8): 939–959, doi:10.1002/joc.670.
- 782 Osborn TJ, Conway D, Hulme M, Gregory JM, Jones PD. 1999. Air flow in-
783 fluences on local climate: observed and simulated mean relationships for the
784 United Kingdom. *Climate Research* **13**(3): 173–191.
- 785 Palin EJ, Scaife AA, Wallace E, Pope EC, Arribas A, Brookshaw A. 2015. Skillful
786 seasonal forecasts of winter disruption to the UK transport system. *J. Appl.*
787 *Meteor. Climatol* doi:10.1175/JAMC-D-15-0102.1.
- 788 Parry S, Marsh T, Kendon M. 2013. 2012: from drought to floods in England
789 and Wales. *Weather* **68**(10): 268–274.
- 790 Scaife A, Arribas A, Blockley E, Brookshaw A, Clark R, Dunstone N, Eade
791 R, Fereday D, Folland C, Gordon M, Hermanson L, Knight JR, Lea DJ,
792 MacLachlan C, Maidens A, Martin M, Peterson AK, Smith D, Vellinga M,
793 Wallace E, Waters J, Williams A. 2014. Skillful long-range prediction of Euro-
794 pean and North American winters. *Geophysical Research Letters* **41**(7): 2514–
795 2519, doi:10.1002/2014GL059637.

Table 1: Average total precipitation (mm) in winter and summer seasons, along with regional correlation with NS and SEE regional precipitation in the two seasons, for HadUKP regions in years 1931–2012. Correlations in bold are significant at the 95% level, based on a two-tailed t-test.

Region	DJF precipitation	NS DJF correlation	SEE DJF correlation	JJA precipitation	NS JJA correlation	SEE JJA correlation
NS	497.3	1	0.13	327.3	1	0.21
SS	410.6	0.88	0.32	299.3	0.75	0.48
ES	200.8	0.44	0.65	204.2	0.50	0.65
NI	286.9	0.52	0.57	251.3	0.56	0.62
NWE	278.0	0.67	0.61	245.6	0.50	0.67
NEE	207.6	0.11	0.79	200.4	0.31	0.71
SWE	314.5	0.34	0.91	212.8	0.43	0.81
CE	158.9	0.05	0.90	175.6	0.20	0.89
SEE	198.0	0.13	1	168.4	0.21	1

- 796 Sibley A, Cox D, Tittley H. 2015. Coastal flooding in England and Wales from
797 Atlantic and North Sea storms during the 2013/2014 winter. *Weather* **70**(2):
798 62–70.
- 799 Svensson C, Brookshaw A, Scaife A, Bell V, Mackay J, Jackson C, Han-
800 naford J, Davies H, Arribas A, Stanley S. 2015. Long-range forecasts of
801 UK winter hydrology. *Environmental Research Letters* **10**(6): 064006, doi:
802 10.1088/1748-9326/10/6/064006.
- 803 Turnpenny JR, Crossley JF, Hulme M, Osborn TJ. 2002. Air flow influences
804 on local climate: comparison of a regional climate model with observa-
805 tions over the united kingdom. *Climate Research* **20**(3): 189–202, URL
806 <http://www.jstor.org/stable/24866806>.
- 807 Wallace J, Lau NC. 1985. On the role of barotropic energy conversions in the
808 general circulation. *Advances in geophysics* **28**: 33–74.
- 809 Weston KJ, Roy MG. 1994. The directional-dependence of the enhancement of
810 rainfall over complex orography. *Meteorological Applications* **1**(3): 267–275.
- 811 Wilby R, O’Hare G, Barnsley N. 1997. The north atlantic oscillation and british
812 isles climate variability, 1865–1996. *Weather* **52**(9): 266–276.
- 813 Wilks DS. 1995. *Statistical methods in the atmospheric sciences*. Academic
814 Press.
- 815 Woollings T, Hannachi A, Hoskins B. 2010. Variability of the north atlantic
816 eddy-driven jet stream. *Quarterly Journal of the Royal Meteorological Society*
817 **136**(649): 856–868, doi:10.1002/qj.625.

Table 2: Regression coefficients for the estimated precipitation anomaly in each region, as given by equation 1. Values in italics are those that fail the significance testing ($p > 0.1$) so are set to zero in the regression equation.

Region	α	β
NS	<i>-21.31</i>	106.32
SS	-26.73	70.81
ES	-31.40	<i>6.45</i>
NI	-34.69	14.80
NWE	-42.74	31.27
NEE	-38.33	<i>-8.00</i>
SWE	-71.87	<i>16.41</i>
CE	-37.08	<i>-6.04</i>
SEE	-56.11	<i>0.60</i>

Table 3: Brier skill scores for precipitation in each HadUKP region obtained from GloSea5 hindcasts of MSLP using the linear regression method, for the period 1992–2011. The two columns show the unadjusted and RPC-adjusted forecasts.

Region	Uncorrected	RPC-corrected
NS	0.21	0.36
SS	0.14	0.28
ES	-0.04	-0.16
NI	0.14	0.25
NWE	0.21	0.33
NEE	0.13	0.14
SWE	0.05	-0.04
CE	0.13	0.19
SEE	0.13	0.09